Cell Reports Medicine, Volume *4*

Supplemental information

Targeting phenylpyruvate restrains excessive NLRP3 inflammasome activation and pathological inflammation in diabetic wound healing

Dongming Lv, Xiaoling Cao, Li Zhong, Yunxian Dong, Zhongye Xu, Yanchao Rong, Hailin Xu, Zhiyong Wang, Hao Yang, Rong Yin, Miao Chen, Chao Ke, Zhicheng Hu, Wuguo Deng, and Bing Tang

Supplemental Figure 1

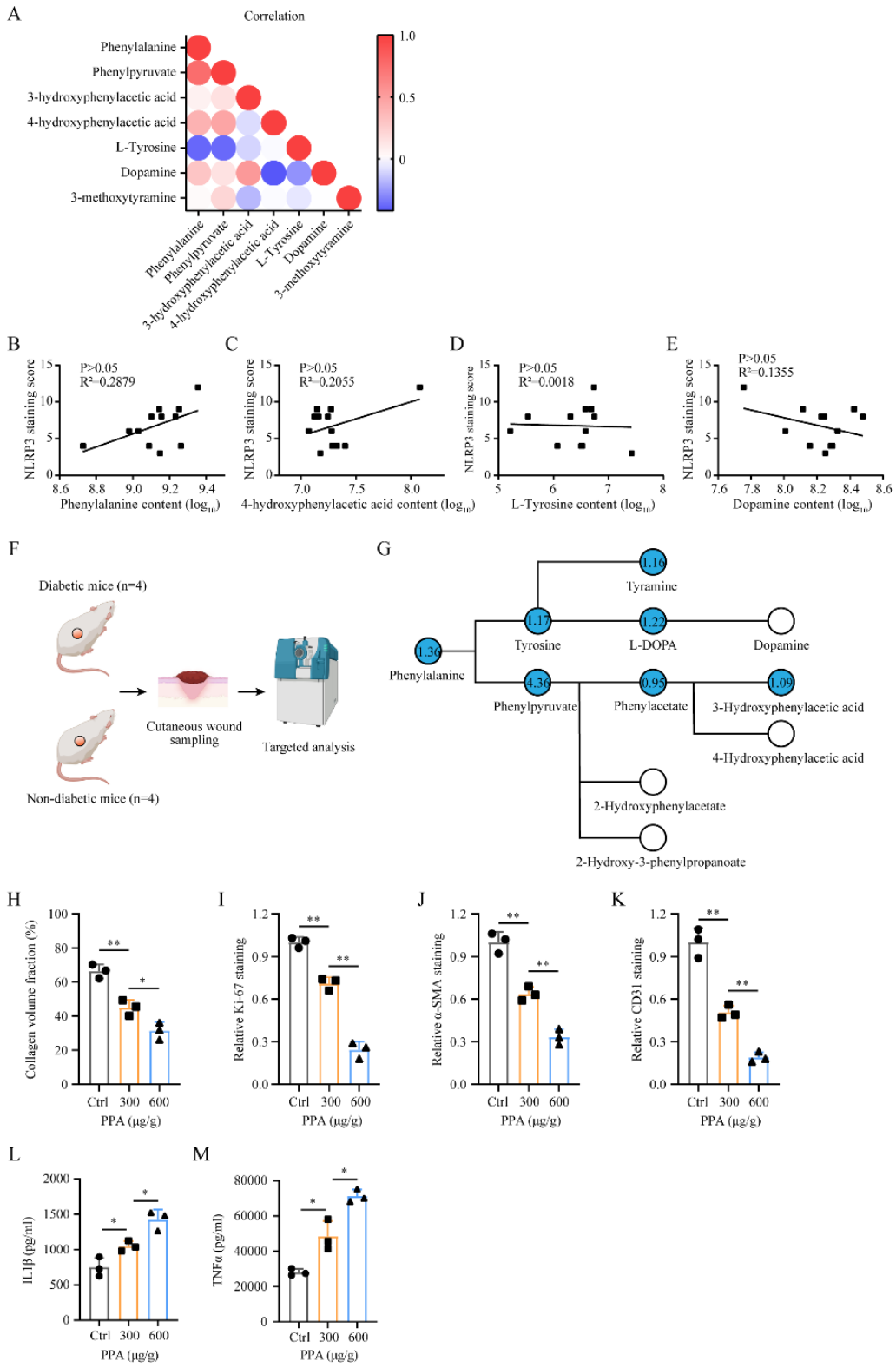

Figure S1. Phenylpyruvate is associated with delayed wound healing and prolonged inflammation. Related to Figure 1. (A) Correlation analysis among differential metabolites in the phenylalanine, tyrosine and tryptophan biosynthesis pathways from comparison of DFU group and NDW group. The colors indicate the values of Pearson r. **(B-E)** Correlation analysis between differential metabolites in the phenylalanine, tyrosine and tryptophan biosynthesis pathways and NLRP3 expression in DFUs (n=12). **(F)** Schematic representation of targeted metabolite analysis in diabetic wounds and nondiabetic wounds. **(G)** Targeted analysis of phenylalanine pathway metabolites. The numbers indicate the fold change in diabetic wounds compared to nondiabetic wounds. Values larger than one suggest upregulation, whereas values smaller than one suggest downregulation in diabetic wounds. White indicates no detection. **(H-K)** Statistical analysis of collagen volume fraction, Ki-67, α-SMA, and CD31 staining in cutaneous wounds (n=3). **(L, M)** ELISA analysis of inflammatory factors, including IL1β and TNFα, in cutaneous wounds on day 6 (n=3). Data are shown as mean ± SD. *P<0.05, **P<0.01.

Supplemental Figure 2

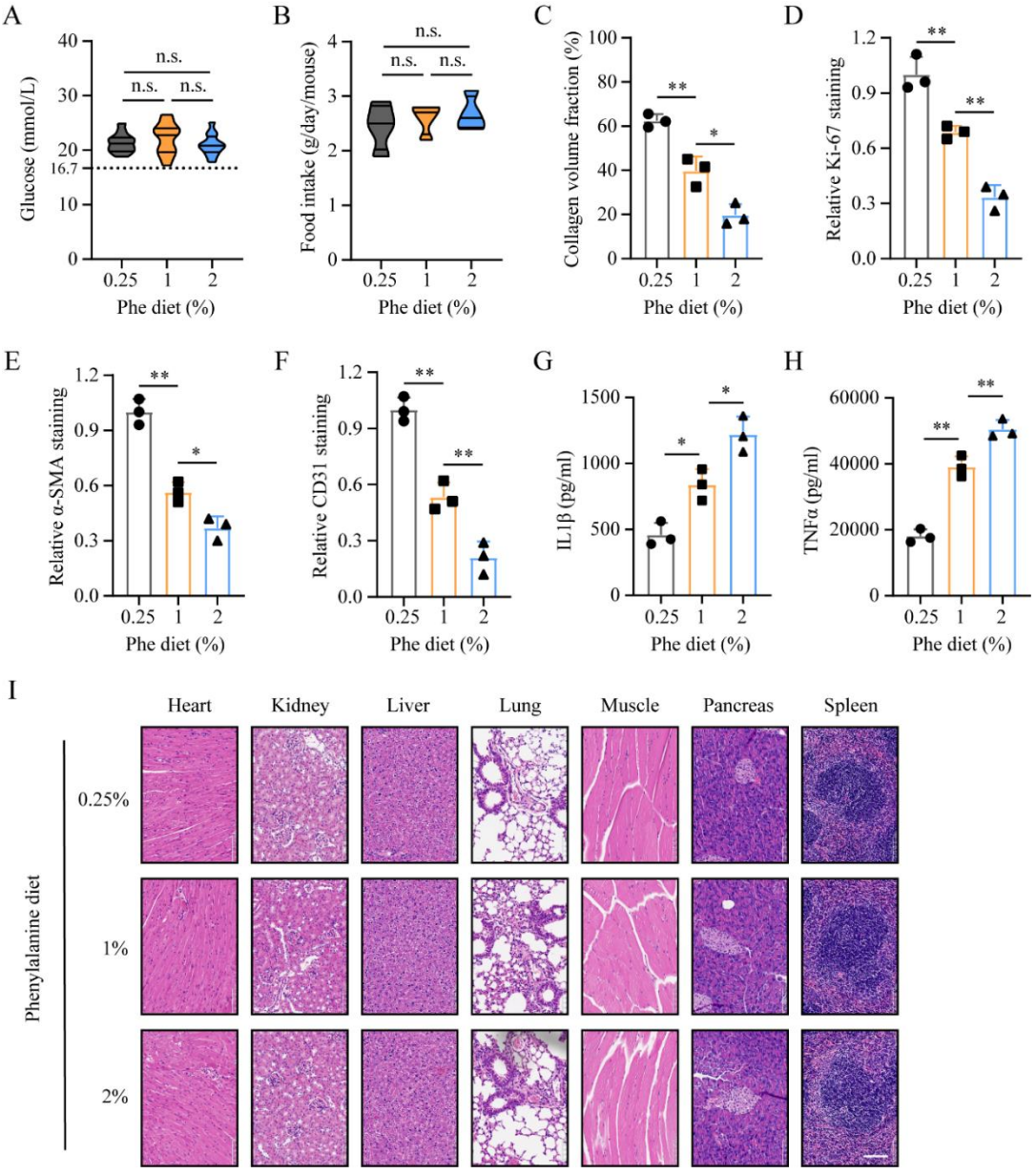

Figure S2. Dietary phenylalanine restriction increases wound healing but has no obvious effect on the general physiological condition *in vivo*. Related to Figure 2. (A, B) Peripheral blood glucose levels and food intake of diabetic mice fed different phenylalanine diets (n=12). **(C-F)** Statistical analysis of collagen volume fraction, Ki-67, α-SMA, and CD31 staining in cutaneous wounds from different groups (n=3). **(G, H)** ELISA analysis of inflammatory factors, including IL1β and TNFα, in cutaneous wounds on day 8 (n=3). **(I)** Representative images of H&E staining of various organs from mice fed different phenylalanine diets. Scale bar: 100 μm. Data are shown as mean ± SD. *P<0.05, **P<0.01; n.s., not significant.

Supplemental Figure 3

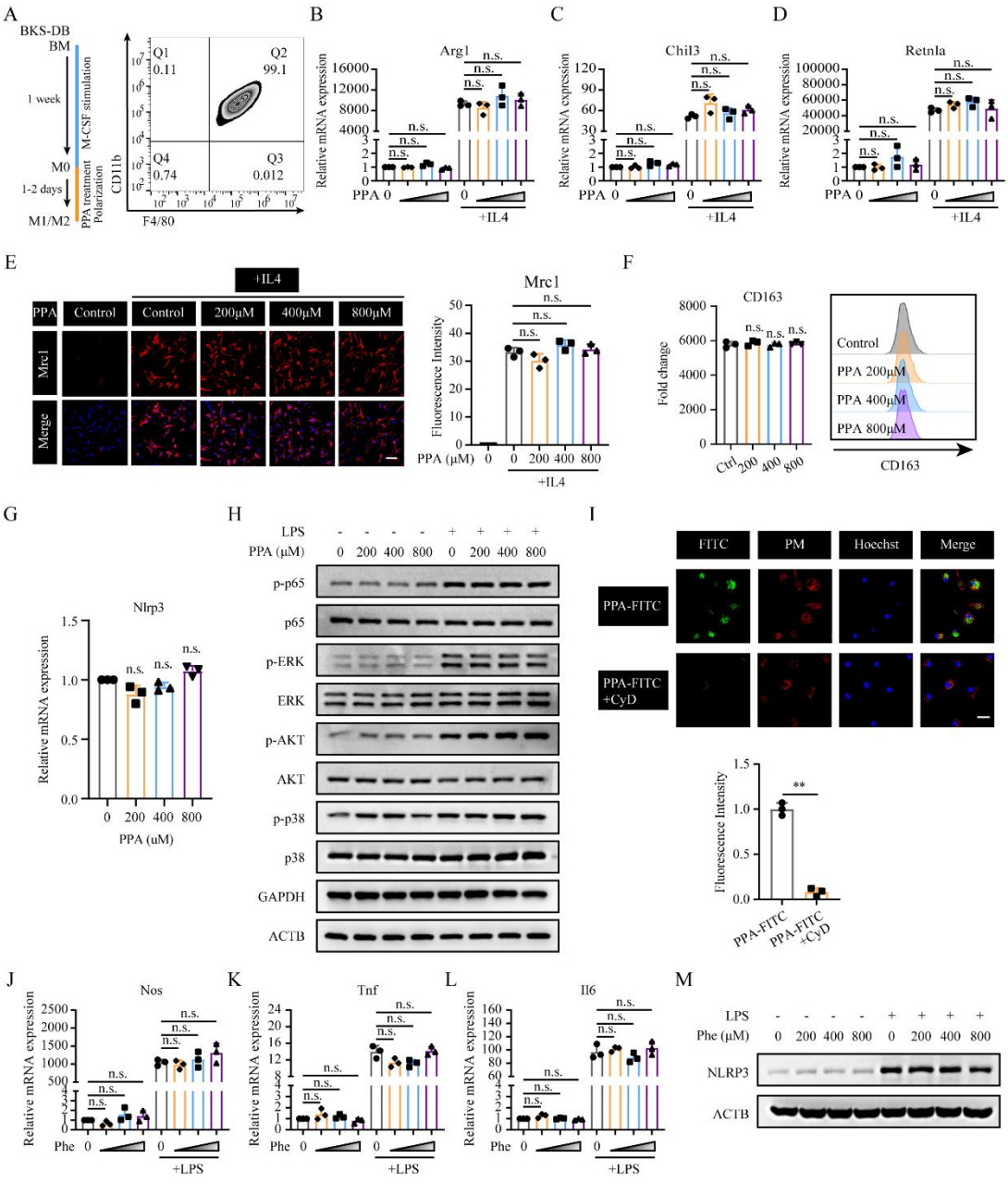

Figure S3. The effect of phenylpyruvate on macrophages. Related to Figure 3. (A) Experimental diagram of macrophage acquisition and polarization. Flow cytometry data showing the identification of macrophage acquisition. **(B-D)** BMDMs were pretreated with DMSO (control) or increasing concentrations of phenylpyruvate for 4 h and then stimulated with media or IL4 (20 ng/mL) for 24 h. The black triangle indicates increasing phenylpyruvate concentrations (PPA) starting from the left: 200, 400, and 800 μM. The RT–qPCR results showing relative mRNA expression of *Arg1*, *Chil3*, and *Retnla*

normalized to *Actb* (n=3). **(E)** Immunostaining and statistical analysis of Mrc1 in BMDMs after pretreatment with phenylpyruvate and stimulation with IL4 (n=3). Scale bar: 150 μm. **(F)** BMDMs were treated as in (B). Flow cytometry data for the M2 surface marker CD163, showing mean fluorescence intensity (MFI) (left) and representative histograms of CD163 (right) (n=3). **(G)** RT–qPCR assay showing the relative NLRP3 mRNA expression after treatment with phenylpyruvate (n=3). **(H)** Immunoblot analysis of BMDMs pretreated with increasing phenylpyruvate concentrations and then stimulated with media or LPS (100 ng/mL) with antibodies recognizing phosphorylated p65, total p65, phosphorylated ERK1/2, total ERK1/2, phosphorylated Akt, total Akt, phosphorylated p38, total p38, GAPDH and ACTB (n=3). **(I)** Immunostaining and statistical analysis showing the uptake of phenylpyruvate into BMDMs, which were pretreated with phenylpyruvate (400 μM) with or without cytochalasin D (10 μM) (n=3). Scale bar: 50 μm. **(J-L)** BMDMs were pretreated with dimethyl sulfoxide (DMSO, control) or increasing concentrations of phenylalanine for 4 h and then stimulated with media or LPS (100 ng/mL) for 24 h. The black triangle indicates increasing phenylalanine concentrations starting from the left: 200, 400, and 800 μM. The RT–qPCR results showing relative mRNA expression of *Nos*, *Tnf*, and *Il6* normalized to *Actb* (n=3). **(M)** Immunoblot analysis of NLRP3 protein levels in BMDMs pretreated with increasing phenylalanine concentrations (n=3). Data are shown as mean ± SD. **P<0.01; n.s., not significant.

Supplemental Figure 4

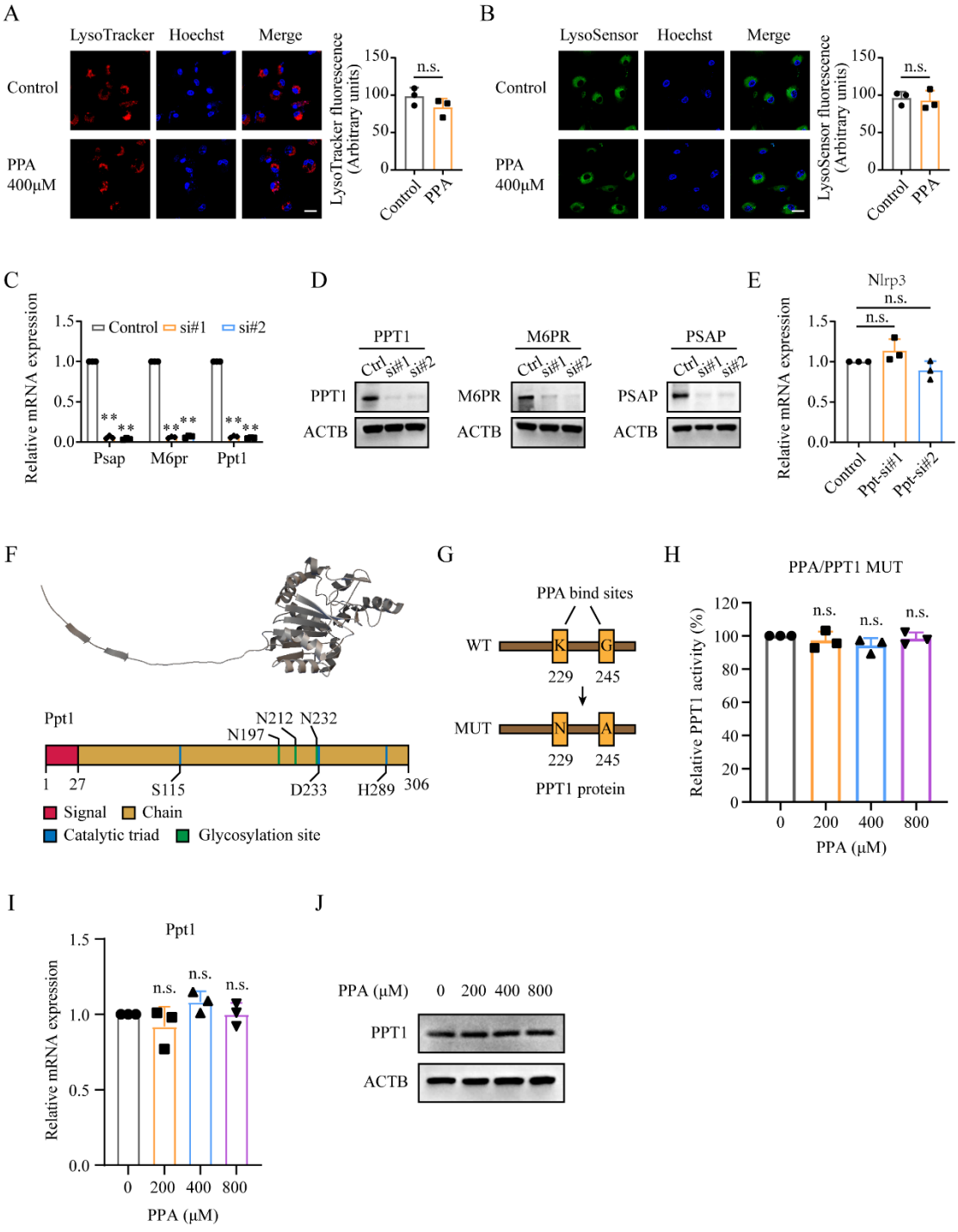

Figure S4. Identification of PPT1 as a target of phenylpyruvate. Related to Figure 4. (A) Immunostaining and statistical analysis of LysoTracker in BMDMs treated with phenylpyruvate (n=3). Scale bar: 50 μm. **(B)** Immunostaining and statistical analysis of LysoSensor in BMDMs treated with phenylpyruvate (n=3). Scale bar: 50 μm. **(C)** RT–qPCR results of Psap, M6pr, and Ppt1 mRNA

expression in BMDMs after knockdown of Psap, M6pr, and Ppt1, respectively (n=3). **(D)** Immunoblot results of Psap, M6pr, and Ppt1 mRNA expression in BMDMs after knockdown of Psap, M6pr, and Ppt1, respectively (n=3). **(E)** RT–qPCR results showing Nlrp3 mRNA expression in BMDMs after knockdown of Ppt1 (n=3). **(F)** A schematic showing the PPT1 protein structure. **(G)** A mutation of the binding site between PPT1 and phenylpyruvate was established based on the autodocking results. **(H)** Enzymatic activity measurement of PPT1 MUT protein coincubated with increasing phenylpyruvate concentrations (n=3). **(I)** RT–qPCR results showing Ppt1 mRNA expression in BMDMs treated with increasing phenylpyruvate concentrations (n=3). **(J)** Immunoblot analysis of PPT1 expression in BMDMs treated with increasing phenylpyruvate concentrations (n=3). Data are shown as mean ± SD. **P<0.01; n.s., not significant.

Supplemental Figure 5

A

ID	Position	Peptide	Score	Cutoff
NLRP3_MOUSE	6	**MTSVRCKLAQYLE	39.746	4.222
NLRP3_MOUSE	405	NEVLFTMCFIPLVCW	6.612	4.222
NLRP3_MOUSE	783	RCGLSHQCCFDISSV	4.135	3.419
NLRP3_MOUSE	784	CGLSHQCCFDISSVL	4.522	4.222
NLRP3_MOUSE	834	QKLWLVSCCLTSACC	7.581	3.419
NLRP3_MOUSE	835	KLWLVSCCLTSACCQ	4.498	4.222
NLRP3_MOUSE	840	SCCLTSACCQDLALV	7.106	3.419
NLRP3_MOUSE	841	CCLTSACCQDLALVL	6.242	4.222

ID	Position	Peptide	Score	Cutoff
NLRP3_RAT	8	MKMMSVRCKLAQYLE	37.94	4.222
NLRP3_RAT	407	NEILFTMCFIPLVCW	6.432	4.222
NLRP3_RAT	786	CGLTHQCCFNISSVL	4.275	4.222
NLRP3_RAT	836	QKLWLVSCCLTSACC	7.581	3.419
NLRP3_RAT	837	KLWLVSCCLTSACCQ	4.674	4.222
NLRP3_RAT	842	SCCLTSACCQDLALV	7.106	3.419
NLRP3_RAT	843	CCLTSACCQDLALVL	6.242	4.222

ID	Position	Peptide	Score	Cutoff
NLRP3_HUMAN	8	MKMASTRCKLARYLE	35.677	4.222
NLRP3_HUMAN	279	LGDLIMSCCPDPNPP	10.37	3.419
NLRP3_HUMAN	280	GDLIMSCCPDPNPPI	6.36	4.222
NLRP3_HUMAN	409	NEVLFTMCFIPLVCW	4.409	4.222
NLRP3_HUMAN	786	RCGLSHECCFDISLV	4.182	3.419
NLRP3_HUMAN	787	CGLSHECCFDISLVL	4.412	4.222
NLRP3_HUMAN	837	KKLWLVSCCLTSACC	5.748	3.419
NLRP3_HUMAN	838	KLWLVSCCLTSACCQ	4.768	4.222
NLRP3_HUMAN	843	SCCLTSACCQDLASV	6.111	3.419
NLRP3_HUMAN	844	CCLTSACCQDLASVL	6.215	4.222
NLRP3_HUMAN	957	NCNLTSHCCWDLSTL	4.338	3.419
NLRP3_HUMAN	958	CNLTSHCCWDLSTLL	4.791	4.222
NLRP3_HUMAN	990	DLGVMMFCEVLKQQS	4.501	4.222

ID	Position	Peptide	Score	Cutoff
NLRP3_MACMU	8	MKMASTRCKLARYLE	35.68	4.222
NLRP3_MACMU	279	LGDLIMSCCPDPNPP	10.42	3.419
NLRP3_MACMU	280	GDLIMSCCPDPNPPI	6.264	4.222
NLRP3_MACMU	409	NEVLFTMCFIPLVCW	4.409	4.222
NLRP3_MACMU	786	CGLSHECCFDISLVL	4.443	4.222
NLRP3_MACMU	836	KKLWLVSCCLTSACC	6.046	3.419
NLRP3_MACMU	837	KLWLVSCCLTSACCQ	4.768	4.222
NLRP3_MACMU	842	SCCLTSACCQDLASV	6.048	3.419
NLRP3_MACMU	843	CCLTSACCQDLASVL	6.215	4.222
NLRP3_MACMU	956	NCNLTSHCCWDLSTL	4.338	3.419
NLRP3_MACMU	957	CNLTSHCCWDLSTLL	4.791	4.222
NLRP3_MACMU	989	DLGVMMFCEVLKQQS	4.501	4.222

ID	Position	Peptide	Score	Cutoff
NLRP3_BOVIN	8	MRMVSVRCKLARYLE	37.395	4.222
NLRP3_BOVIN	276	LGDLIASCCPGPNPP	10.332	3.419
NLRP3_BOVIN	277	GDLIASCCPGPNPPI	4.773	4.222
NLRP3_BOVIN	406	NEILFTMCFIPLVCW	5.028	4.222
NLRP3_BOVIN	775	RRLWLGQCCLSHQCC	6.694	3.419
NLRP3_BOVIN	781	QCCLSHQCCFNISSV	4.063	3.419
NLRP3_BOVIN	832	KKLWLVSCCLTSASC	4.729	3.419
NLRP3_BOVIN	833	KLWLVSCCLTSASCE	4.775	4.222
NLRP3_BOVIN	952	NCSLTSHCCWDLSTL	4.919	3.419
NLRP3_BOVIN	953	CSLTSHCCWDLSTLL	4.402	4.222
NLRP3_BOVIN	985	DLGVMLLCEVLKQQG	4.298	4.222

B

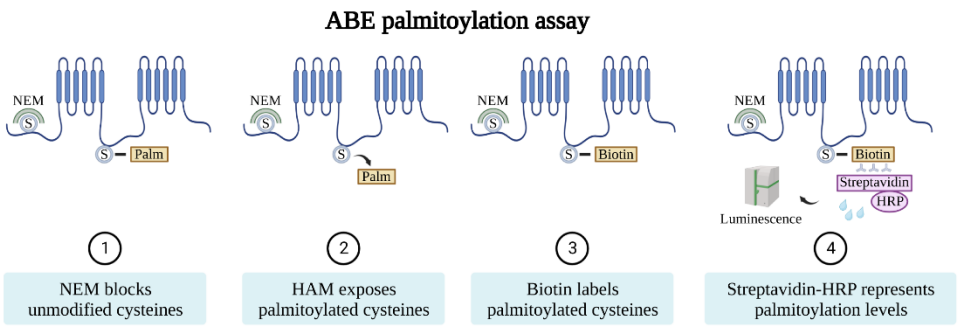

C

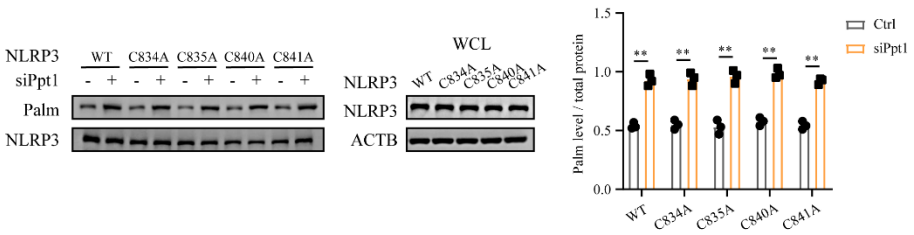

Figure S5. Identification of the palmitoylation site of NLRP3. Related to Figure 5. (A) Alignment of NLRP3 sequences containing predicted palmitoylation sites among different species. **(B)** A schematic illustrating the general process of the ABE palmitoylation assay. **(C)** MEFs were transfected

with wild-type (WT) NLRP3 or the indicated NLRP3 mutants for 24 h with or without knockdown of Ppt1. ABE assay and immunoblot analysis showing palmitoylation levels of the indicated NLRP3 mutants (n=3). Data are shown as mean ± SD. **P<0.01.

Supplemental Figure 6

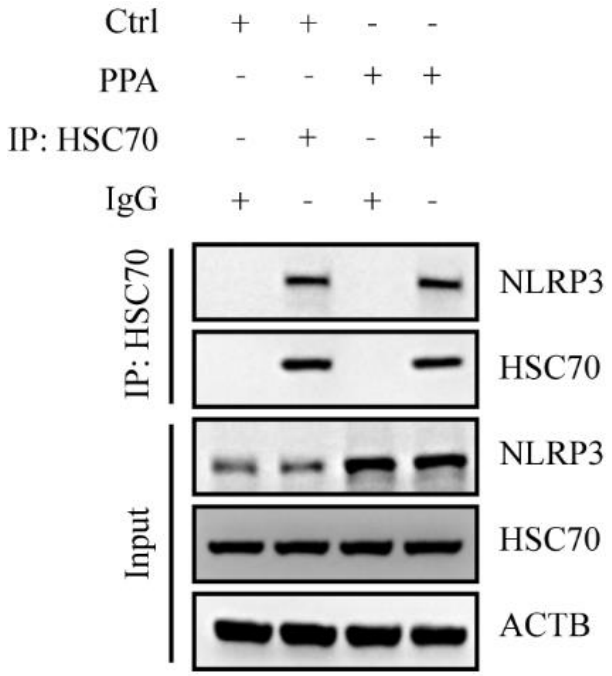

Figure S6. BMDMs were treated with phenylpyruvate (400 μM) for 4 h and LPS (100 ng/mL) for 24 h and then stimulated with ATP (3 mM) for 45 min. Cell lysates were collected to determine the interaction between NLRP3 and HSC70 by immunoprecipitation (IP) and immunoblot analysis (n=3), Related to Figure 6.

Supplemental Figure 7

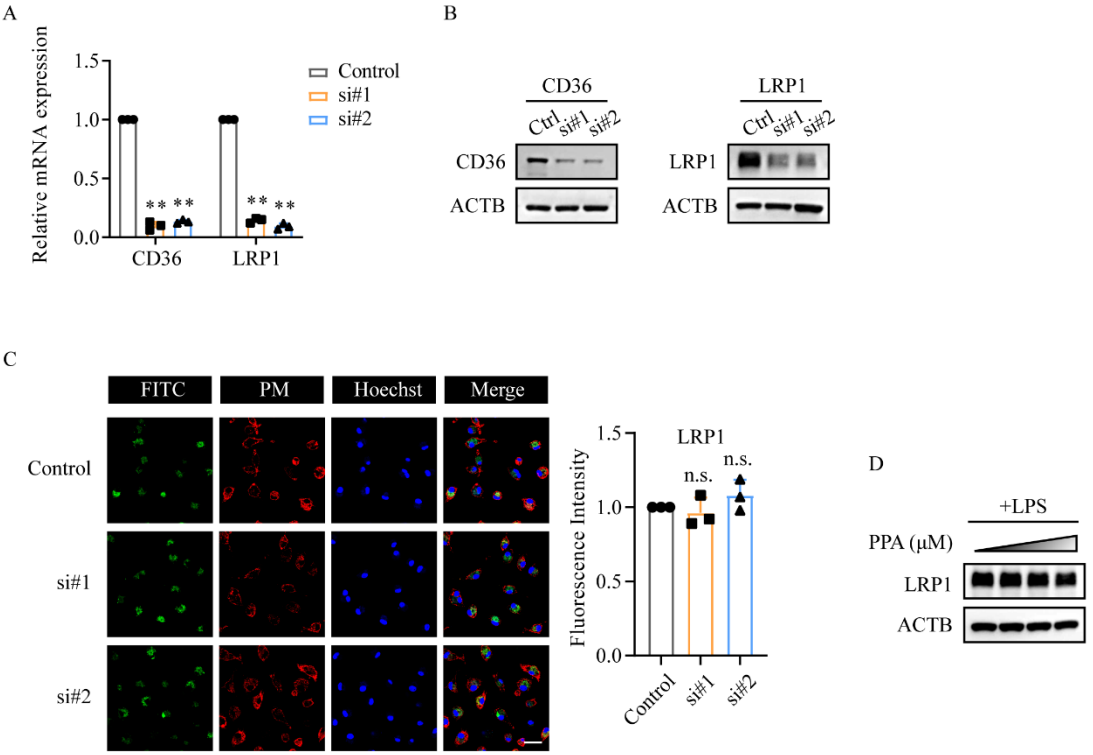

Figure S7. Identification of CD36-mediated phenylpyruvate uptake in macrophages. Related to Figure 7. (A) RT–qPCR assay showing relative mRNA expression of CD36 and LRP1 in BMDMs with knockdown of CD36 and LRP1, respectively (n=3). **(B)** Immunoblot analysis of CD36 and LRP1 expression in BMDMs with knockdown of CD36 and LRP1, respectively (n=3). **(C)** Immunostaining and statistical analysis showing the uptake of phenylpyruvate in BMDMs with or without knockdown of LRP1. The FITC antibody indicated phenylpyruvate, and the lipid raft antibody indicated plasma membrane (n=3). Scale bar: 50 μm. **(D)** Immunoblot analysis of total LRP1 protein expression in BMDMs treated with increasing phenylpyruvate concentrations. The black triangle indicates increasing phenylpyruvate concentrations starting from the left: 200, 400, and 800 μM (n=3). Data are shown as mean ± SD. **P<0.01; n.s., not significant.